EC Journals.ASM.org

Cryptococcus neoformans Dual GDP-Mannose Transporters and Their Role in Biology and Virulence

Zhuo A. Wang,[a] Cara L. Griffith,[a]* Michael L. Skowyra,[a]* Nichole Salinas,[a] Matthew Williams,[a] Ezekiel J. Maier,[c,d] Stacey R. Gish,[a] Hong Liu,[a]* Michael R. Brent,[b,c,d] Tamara L. Doering[a]

Departments of Molecular Microbiology[a] and Genetics[b] and The Center for Genome Sciences,[c] Washington University School of Medicine, St. Louis, Missouri, USA; Department of Computer Science, Washington University, St. Louis, Missouri, USA[d]

Cryptococcus neoformans **is an opportunistic yeast responsible for lethal meningoencephalitis in humans. This pathogen elaborates a polysaccharide capsule, which is its major virulence factor. Mannose constitutes over one-half of the capsule mass and is also extensively utilized in cell wall synthesis and in glycosylation of proteins and lipids. The activated mannose donor for most biosynthetic reactions, GDP-mannose, is made in the cytosol, although it is primarily consumed in secretory organelles. This compartmentalization necessitates specific transmembrane transporters to make the donor available for glycan synthesis. We previously identified two cryptococcal GDP-mannose transporters, Gmt1 and Gmt2. Biochemical studies of each protein expressed in *Saccharomyces cerevisiae* showed that both are functional, with similar kinetics and substrate specificities *in vitro*. We have now examined these proteins *in vivo* and demonstrate that cells lacking Gmt1 show significant phenotypic differences from those lacking Gmt2 in terms of growth, colony morphology, protein glycosylation, and capsule phenotypes. Some of these observations may be explained by differential expression of the two genes, but others suggest that the two proteins play overlapping but nonidentical roles in cryptococcal biology. Furthermore, *gmt1 gmt2* double mutant cells, which are unexpectedly viable, exhibit severe defects in capsule synthesis and protein glycosylation and are avirulent in mouse models of cryptococcosis.**

Mannose is a dominant component of fungal glycoconjugates, in contrast to its lesser role in parallel structures of higher organisms. For example, in both mammals and fungi N-glycosylation of proteins begins with the transfer to asparagine of a conserved structure consisting of two *N*-acetylglucosamine and eight mannose residues in the endoplasmic reticulum. Mammals typically process this initial structure to forms with only three mannose residues, elaborating the modified core with other moieties such as galactose, *N*-acetylglucosamine, and N-acetylneuraminic acid in the Golgi apparatus (1). In contrast, yeasts maintain most or all of the initial mannose-rich structure and frequently elaborate it to various extents with additional mannose residues, ranging from the relatively limited elongation seen in *C. neoformans* to the extensive modifications observed in *Saccharomyces cerevisiae* (2, 3). As another example, mammalian O-glycans typically contain fucose, xylose, and *N*-acetylglucosamine (1). In contrast, fungal O-glycans are initiated by the addition of mannose to serine/threonine residues and are generally elongated with several more mannoses (2, 4). Proteins extensively modified with mannose (mannoproteins) are important constituents of fungal cell walls, so that mannose constitutes 30 to 50% of the cell wall mass of the model yeast *S. cerevisiae* (5). Mannose further occurs as a component of fungal glycolipids (2), GPI anchors (6), and capsules (see below).

Glycan biosynthetic reactions require high-energy monosaccharide donors; in the case of mannose, this compound is the nucleotide sugar GDP-mannose. Its synthesis is catalyzed by the action of GDP-mannose phosphorylase on GTP and mannose-1-phosphate; the latter is generated in the cytosol from mannose-6-P (7). Some GDP-mannose is used at the cytosolic face of the endoplasmic reticulum (ER) to form lipid-linked oligosaccharide precursors of N-glycans (7) or dolichol-P-mannose. These products are subsequently flipped into the ER for further modification or for use as mannose donors in glycosylation reactions, respectively (8). Most GDP-mannose, however, is used as a substrate for glycosylation reactions in the lumen of the Golgi complex (7). To enter the Golgi, this negatively charged compound requires a specific nucleotide sugar transporter (9, 10). GDP-mannose transport activity was first identified and characterized through *in vitro* studies of *S. cerevisiae* (11). *VRG4*, the gene encoding the GDP-mannose transporter, was subsequently identified in *S. cerevisiae* (12, 13) and other fungi (see below). GDP-mannose transporters have also been reported in plants (14–16) and the protozoan parasite *Leishmania donovani* (17, 18). Notably, mammalian cells lack GDP-mannose transporters, since they do not perform mannosylation in the Golgi.

As expected from its role in GDP-mannose transport, the *S. cerevisiae* Vrg4 protein is localized to the Golgi apparatus and required for normal Golgi functions (12, 13); the corresponding *VRG4* gene is essential (12). Viable cells that express partly functional mutant Vrg4 have been reported, but these strains show defects in both N- and O-linked protein glycosylation and are more sensitive than their wild-type counterparts to cell wall stress (12, 13, 19). Single *VRG4* homologs have been identified in multiple fungi, including *Pichia pastoris* (20), *Aspergillus niger* (21),

Received 24 February 2014 **Accepted** 17 April 2014

Published ahead of print 18 April 2014

Address correspondence to Tamara L. Doering, doering@wustl.edu.

* Present address: Cara L. Griffith and Hong Liu, Monsanto Corporation, St. Louis, Missouri, USA; Michael L. Skowyra, Department of Cell Biology, Washington University School of Medicine, St. Louis, Missouri, USA.

Supplemental material for this article may be found at http://dx.doi.org/10.1128/EC.00054-14.

doi:10.1128/EC.00054-14

Aspergillus fumigatus (22), *Candida glabrata* (23), and *Candida albicans* (24); all of them complement *S. cerevisiae vrg4* mutants. While most of these genes, like the *S. cerevisiae VRG4* gene, are essential, it is notable that *A. fumigatus* cells lacking GmtA are viable although significantly impaired (22). The GDP-mannose transporter of the protozoan parasite *L. donovani* is also not essential for cell viability, although it is required for parasite virulence (17, 18). Finally, the *Aspergillus nidulans* genome contains two *VRG4*-like genes, *gmtA* and *gmtB* (25). Both of these are thought to encode functional GDP-mannose transporters since the reduced cell surface mannosylation of a *gmtA* mutant can be corrected by overexpression of *gmtB* (26); a double mutant has not been reported.

Our studies focus on the encapsulated fungal pathogen *Cryptococcus neoformans*, which causes severe disease in immunocompromised individuals and over 600,000 deaths per year worldwide (27). Pathogenic members of the *Cryptococcus* genus have historically been classified by seroreactivity of their capsule polysaccharides (28); serotypes A and D are the main ones responsible for opportunistic infections. The glycoconjugates of *C. neoformans* include mannose-containing glycoproteins and glycolipids (3, 4, 29, 30). Mannose is also a major component of this organism's extensive polysaccharide capsule (31), which is essential for fungal virulence. The capsule is composed primarily of two polysaccharides, glucuronoxylomannan (GXM) and glucuronoxylomannogalactan (GXMGal; also termed GalXM [28]), along with a small amount of mannoproteins (31). GXM accounts for about 90% of the capsule mass and consists of a mannose backbone modified with xylose, glucuronic acid, and acetyl groups (32). Mutants lacking GXM are avirulent in animal models, suggesting that it plays an important role in pathogenesis (33). We have reported that GXM is made within the secretory pathway (34), which would require the translocation of GDP-mannose into luminal compartments. The second capsule polymer, GXMGal, is less well understood but is also associated with cryptococcal virulence (35). GXMGal is based on a linear polymer of galactose, and its side chains contain mannose residues along with galactose, glucuronic acid, and xylose (36–38).

We previously identified two *C. neoformans* genes encoding GDP-mannose transporters, *GMT1* and *GMT2*, which encode proteins that are 63% identical at the amino acid level (39). Each of these genes effectively complements the *S. cerevisiae vrg4* mutant, and the two proteins demonstrate similar GDP-mannose transport activity *in vitro* (39). Strains lacking either gene are viable, although the mutants do have distinct phenotypes, with *gmt1* cells exhibiting a severe capsule defect while *gmt2* cells produce normal capsules (39). In addition, transcriptional analysis suggests that the two genes are not coordinately regulated and therefore may have distinct biological functions in *C. neoformans* (39).

To investigate potential functional differences between the two cryptococcal GDP-mannose transporters, we generated a double mutant strain and evaluated mannose-related phenotypes of the single and double mutants in comparison to the parental strain. We also assessed phenotypes and *GMT* transcription in strains in which the coding sequence of each gene was expressed from the usual chromosomal location of the other. Finally, we determined that loss of both transporters has significant impact on capsule synthesis and protein glycosylation and completely abrogates fungal virulence.

TABLE 1 *C. neoformans* strains used in these studies

C. neoformans strain[a]	Serotype	Origin
KN99	A	61
KN99 *gmt1*	A	This study
KN99 *gmt2*	A	This study
KN99 *gmt1 gmt2*	A	This study
KN99 *gmt1*::*GMT1*	A	This study
JEC21	D	62
JEC21 *gmt1*	D	39
JEC21 *gmt2*	D	39
JEC21 *gmt1*::*GMT1*	D	39
JEC21 *gmt1 gmt2*	D	This study
JEC21 *gmt1 gmt2*::*GMT1*[b]	D	This study
JEC21 *gmt2 gmt1*::*GMT2*[b]	D	This study
JEC21 *GMT1*-HA	D	4
JEC21 *GMT1*-HA *GMT2*-FLAG	D	This study

[a] All strains are MATα.
[b] In these strains, only the coding region was moved to a new location; flanking regions retained the native sequences.

MATERIALS AND METHODS

Cell growth. All *C. neoformans* strains (Table 1) were grown at 30°C if not otherwise indicated. Cells were cultured in YPD medium (1% [wt/vol] yeast extract, 2% [wt/vol] peptone, 2% [wt/vol] dextrose) with shaking (230 rpm) or grown on YPD agar plates (YPD medium with 2% [wt/vol] agar); for strains marked with drug resistance cassettes, 100 μg/ml nourseothricin (Werner BioAgents) or Geneticin (G418; Invitrogen) and/or 150 μg/ml hygromycin B (Roche) was included in the medium. For immunofluorescence localization, strains were cultured in minimal medium, consisting of 0.17% yeast nitrogen base without amino acids and $(NH_4)_2SO_4$, 0.5% (wt/vol) $(NH_4)_2SO_4$, and 2% (wt/vol) dextrose. To test *C. neoformans* growth in the presence of stressors, cells from an overnight culture were washed, resuspended in water at an optical density at 600 nm (OD_{600})/ml of 1, and diluted 10-fold with YPD medium containing caffeine, sodium dodecyl sulfate (SDS), or hygromycin B to yield the desired concentrations. Aliquots of 100 μl of these suspensions were transferred into a 96-well plate and incubated to follow growth by OD_{600}.

Strain construction (serotype D). To make a *gmt1 gmt2* double mutant, the *gmt2* deletion construct described previously (39) was biolistically transformed into a *gmt1* mutant strain (39). Genomic DNA was extracted from drug-resistant transformants and screened by PCR to confirm replacement of *GMT2* by the appropriate marker. DNA blotting (not shown) confirmed the presence of both gene replacements and the absence of additional ectopic insertions of drug markers.

For Gmt2 localization, the coding sequence of the serotype D gene, designated here *GMT2*(D), was PCR amplified from JEC21 genomic DNA (4) using primers GMT2-1 and GMT2-2 to generate a 2,914-bp *GMT2*(D) DNA fragment, GMT2-3 and GMT2-4 to generate a DNA fragment consisting of the 26-bp FLAG epitope and 336 bp 3′ to the *GMT2* gene, and GMT2-7 and GMT2-8 to generate a 1,142-bp *GMT2*(D) downstream DNA fragment. A 2,821-bp hygromycin resistance cassette was amplified from plasmid $pHYG_7$-KB_1 (40) using primers GMT2-5 and GMT2-6. The four amplicons were next assembled by fusion PCR and cloned into the pCR2.1-TOPO vector (Invitrogen) to form the plasmid pGMT2(D)-Flag-Hyg. To improve transformation efficiency, the hygromycin resistance cassette of pGMT2(D)-Flag-Hyg was replaced by a cassette encoding Geneticin resistance inserted in the opposite orientation from the *GMT2* gene. To do this, the latter cassette was released from pIB103 (41) by digestion with BlpI and AgeI and cloned into BlpI- and AgeI-digested and calf intestinal alkaline phosphatase-treated pGMT2(D)-Flag-Hyg to form the plasmid pGMT2(D)-Flag-G418. To prepare DNA for transformation using a split marker disruption strategy (42), a fragment of DNA containing the *GMT2*-Flag sequence and the 3′ portion of the Geneticin resis-

tance cassette was released from pGMT2(D)-Flag-G418 by digestion with ClaI and SmlI. An overlapping fragment consisting of *GMT2*(D) downstream sequence and the 5′ portion of the Geneticin resistance cassette was released from the same plasmid by digestion with PstI and KpnI. To replace the chromosomal copy of the *GMT2* gene with *GMT2*-Flag, the two overlapping DNA fragments were mixed at an equimolar ratio and biolistically transformed into a strain expressing Gmt1-HA (4). Genomic DNA was prepared from Geneticin-resistant transformants and screened by PCR. Gmt2-Flag protein expression was confirmed by immunostaining.

We wanted to generate strains in which only one *GMT* gene was expressed and that gene was expressed from the opposite locus. To express the coding sequence of *GMT1* from the *GMT2* locus, maintaining the *GMT2* promoter and terminator, we again used fusion PCR and a split marker strategy to modify the *gmt1* strain. We first used JEC21 genomic DNA as a template to amplify a 1,776-bp fragment consisting of the *GMT1*(D) coding sequence with 3′-terminal addition of a 20-bp fragment of the *GMT2*(D) downstream sequence using primers ZAW-117 and ZAW-118; a 910-bp fragment of sequence upstream of *GMT2*(D) using primers ZAW-115 and ZAW-116; and a 937-bp fragment of sequence downstream of *GMT2*(D) using primers ZAW-119 and ZAW-120. We also amplified an 867-bp portion of a nourseothricin resistance cassette with 5′-terminal addition of a 20-bp fragment of the *GMT2*(D) downstream sequence from plasmid pGMC200 (43) using primers ZAW-114 and ZAW-078; an overlapping 1,392-bp fragment of the same cassette was amplified using primers GMT1CB-E and GMT1CB-F. The 1,776-bp, 910-bp, and 851-bp amplicons were next assembled by fusion PCR and cloned into the pCR2.1-TOPO vector (Invitrogen) to form the plasmid pGMT1R2-5; this construct was confirmed by DNA sequencing. The 937-bp and 1,392-bp amplicons were similarly assembled, and the product was mixed at a 1:1 molar ratio with the fragment released by XbaI and SpeI digestion of plasmid pGMT1R2-5. The mixed DNA was biolistically transformed into the serotype D *gmt1* strain as described above. Transformants were identified by nourseothricin resistance and verified by PCR analysis and DNA sequencing (not shown).

To express the coding sequence of *GMT2* from the *GMT1* locus, maintaining the *GMT1* promoter and terminator, we used overlap PCR and a split marker strategy to modify the *gmt2* strain. We used JEC21 genomic DNA as the template to generate a 1,613-bp fragment consisting of the *GMT2*(D) coding sequence with 3′-terminal addition of a 21-bp fragment of the *GMT1*(D) downstream sequence using primers ZAW-128 and ZAW-129, an 820-bp fragment of sequence upstream of *GMT1*(D) using primers ZAW-126 and ZAW-127, and an 841-bp fragment of sequence downstream of *GMT1*(D) using ZAW-134 and ZAW-135. We also amplified a 1,725-bp segment of a Geneticin resistance cassette from plasmid pIB103 (44) with 5′-terminal addition of a 21-bp fragment of *GMT1*(D) downstream sequence using primers ZAW-130 and ZAW-131 and an overlapping 1,554-bp fragment using primers ZAW-132 and ZAW-133. The 1613-bp, 820-bp, and 1,725-bp amplicons were next assembled by fusion PCR and cloned into the pCR2.1-TOPO vector (Invitrogen) to form plasmid pGMT2R1-5; this construct was checked by DNA sequencing. The 841-bp and 1,554-bp amplicons were similarly assembled, and the product was mixed at a 1:1 molar ratio with the fragment released from the plasmid pGMT2R1-5 by digestion with XbaI and SpeI. The mixed DNA was biolistically transformed into the serotype D *gmt2* strain as described above. Transformants were identified by Geneticin resistance and verified by PCR analysis and DNA sequencing (not shown).

Virulence studies (serotype A). For use in mouse infections, mutant strains were generated in the more virulent serotype A background. For *gmt1*, a 1,248-bp fragment upstream of the serotype A gene, designated here *GMT1*(A), was amplified from KN99α genomic DNA using primers Gmt1-7 and Gmt1-4b, and a 1,329-bp fragment downstream of *GMT1*(A) was amplified using primers Gmt1-5b and Gmt1-8. A 2,930-bp hygromycin resistance cassette was amplified from plasmid pHYG$_7$-KB$_1$ using primers Gmt1-3b and Gmt1-6. The three amplicons were next assembled by fusion PCR, and the final construct was biolistically transformed into KN99α cells. For *gmt2*, a 1,295-bp fragment upstream of the serotype A gene, designated here *GMT2*(A), was amplified from KN99α genomic DNA using primers Gmt2-7 and Gmt2-4, and a 1,294-bp fragment downstream of *GMT2*(A) was amplified using primers Gmt2-5b and Gmt2-8. A 1,868-bp nourseothricin resistance cassette was amplified from plasmid pGMC200 using primers Gmt2-3 and Gmt2-6. The three amplicons were next assembled by fusion PCR, and the final construct was biolistically transformed into KN99α cells. Transformed cells were allowed to recover for 24 h on YPD medium, transferred onto YPD plates containing hygromycin or nourseothricin as appropriate, and incubated at 30°C for 3 to 5 days. For the *gmt1 gmt2* double mutant, the *gmt2* deletion construct described above was biolistically transformed into the serotype A *gmt1* mutant strain. For all strains, genomic DNA was extracted from drug-resistant transformants and screened by PCR to confirm replacement of *GMT1*(A) or *GMT2*(A) by the appropriate markers. DNA blotting was used to confirm gene replacements and that any marker cassette was present only once in the genome, with no additional ectopic insertions.

To complement the serotype A *gmt1* strain at the original locus using overlap PCR and a split marker strategy, a 2,819-bp *GMT1*(A) sequence with its flanking sequences was PCR amplified from KN99α genomic DNA using primers GMT1CB-A and GMT1CB-B; a 985-bp fragment of sequence downstream of *GMT1*(A) was amplified from the same DNA using GMT1CB-G and GMT1CB-H. An 851-bp portion of a nourseothricin resistance cassette was amplified from plasmid pGMC200 using primers GMT1CB-C and GMT1CB-D; an overlapping 1,392-bp fragment of the same cassette was amplified using primers GMT1CB-E and GMT1CB-F. The 2,891-bp and 851-bp amplicons were next assembled by fusion PCR and cloned into the pCR2.1-TOPO vector (Invitrogen) to form the plasmid pGMT1CB-5. The 985-bp and 1,392-bp amplicons were similarly assembled and cloned to form the plasmid pGMT1CB-3. The two fused fragments were released from their respective vectors by digestion with XbaI and SpeI, mixed at a 1:1 molar ratio, and biolistically transformed into the disruption strain as described above. Transformants were identified by nourseothricin resistance, and complementation was verified by PCR analysis and reversion of phenotypes (not shown).

Strains to be tested were cultured overnight in YPD medium, collected by centrifugation, washed in phosphate-buffered saline (PBS), and diluted to 2×10^6 cells/ml in PBS. For each strain, 10 4- to 6-week-old female A/Jcr mice (from the National Cancer Institute) were anesthetized with a combination of ketamine hydrochloride (Ketaset) and xylazine and inoculated intranasally with 100 μl of the prepared suspenstion of *C. neoformans*. The animals were weighed the day of inoculation and were sacrificed if weight decreased to a value below 80% of peak weight on any subsequent day (an outcome which in this protocol precedes any signs of disease) or upon completion of the study. Initial inocula were plated to confirm CFU. All studies were performed in compliance with institutional guidelines for animal experimentation.

Immunoblotting. Cells from a 3-ml overnight culture in YPD medium were harvested by centrifugation (2,500 × *g*, 10 min, 4°C) and washed in 500 μl of cold lysis buffer (50 mM Tris-HCl, pH 8.0, 0.1 mM EDTA, and 1% SDS) with protease inhibitors (chymostatin, leupeptin, antipain, and pepstatin A, each at 10 μg/ml final concentration, and 0.2 mM phenylmethylsulfonyl fluoride). The suspension was then vigorously vortex mixed with 200 μl of 0.5-mm glass beads (Biospec Products, Bartlesville, OK) for 1-min intervals alternating with 2 min on ice until ~80% breakage was observed under a light microscope. The lysate was centrifuged (6,000 × *g*, 1 min, at room temperature [RT]), and the supernatant was reserved. Protein concentration of each sample was determined by Bio-Rad protein assay (Bio-Rad). Equal amounts of protein from each fraction were boiled in SDS-PAGE sample buffer and resolved by SDS-PAGE on a 12% gel. Standard methods were used for transfer and immunoblotting, using dilutions of 1:1,000 for rabbit polyclonal anti-α-1,6-mannose antibody (45) and rabbit polyclonal anti-cell wall protein antibody (CWP) (46), and 1:5,000 for chicken polyclonal anti-β-elimi-

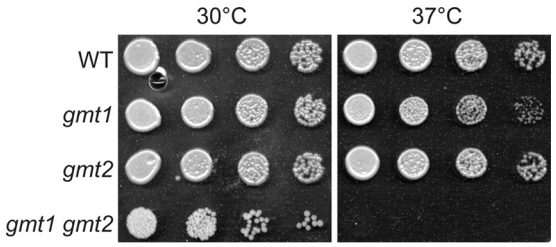

FIG 1 Temperature sensitivity of *gmt* mutants. Aliquots of 5 μl of a stock cell suspension (OD_{600} = 0.1) and three 5-fold serial dilutions were spotted on YPD plates containing 80 μg/ml calcofluor white and grown for 5 days at the temperatures shown. Strains used in all figures are in the serotype D JEC21 background unless indicated otherwise. WT, wild type.

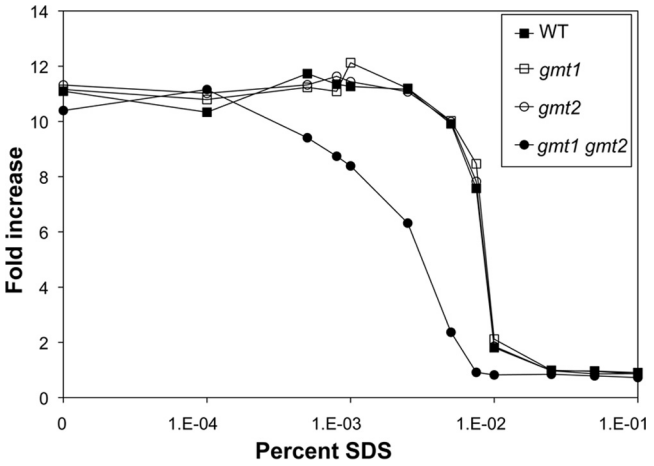

FIG 2 Mutants lacking both *GMT1* and *GMT2* are sensitive to cell stress. Growth at 24 h, measured as fold increase compared to the starting culture, is plotted as a function of SDS concentration in the medium. The double mutant (filled circles) is highly sensitive to SDS compared to wild-type and single mutant strains.

nated mannoprotein antibody (from S. Levitz, Boston University School of Medicine, Boston, MA) and secondary antibodies (anti-chicken IgG conjugated to horseradish peroxidase from Sigma; anti-rabbit IgG conjugated to horseradish peroxidase from GE Healthcare). Detection was with the Western Lighting chemiluminescence reagent (PerkinElmer Life Sciences).

Capsule induction. For capsule induction, single colonies were inoculated into 50 ml of YPD medium and shaken overnight at 30°C. Approximately 10^8 cells were collected by centrifugation (2,500 × *g*, 10 min, 4°C), washed twice with 1 ml Dulbecco's modified Eagle medium (DMEM; Sigma), and resuspended in DMEM at 10^6/ml. The washed cell suspension was then transferred into a 24-well tissue culture plate (TPP; 1 ml/well) and incubated at 37°C in a 5% CO_2 atmosphere. After 48 h, the cells were collected by centrifugation, resuspended in 8 μl PBS, and mixed with 1.5 μl India ink. A 5-μl volume of the suspension was spotted onto a microscope slide, and cells were viewed with a ZEISS Axioskop2 MOT Plus microscope (Carl Zeiss, Thornwood, NJ) with a 40× objective. Random fields were photographed and printed for manual measurement of capsule radius and cell diameter.

RNA-Seq. Wild-type cells were cultured overnight in YPD followed by growth in capsule-inducing conditions (DMEM, 37°C, 5% CO_2), RNA isolation, and transcriptome sequencing (RNA-Seq) analysis as described in reference 47. RNA was isolated at 0, 1.5, 3, 8, and 24 h of culture.

qRT-PCR. For quantitative reverse transcriptase PCR (qRT-PCR), cells were cultured overnight in YPD and then either harvested directly or grown under capsule-inducing conditions as above for 3 h. RNA was prepared from 10^8 cells and analyzed as described in reference 39 using the following primers: ZAW-117 and ZAW-166 for *GMT1*; ZAW-063 and ZAW-137 for *GMT2*; and ZAW-171 and ZAW-172 for *ACT1* (for normalization).

Microscopy. Capsule immunofluorescence was performed as described in reference 39 using 50 μg/ml anti-capsular monoclonal antibody 3C2 (from T. Kozel, University of Nevada at Reno) followed by 200 ng/ml of Alexa Fluor 488-tagged anti-mouse antibody (Invitrogen). Transmission electron microscopy was performed exactly as described in reference 48.

For protein localization, sample preparation for microscopy was done as described in reference 4. After blocking, slides were treated with either a high-affinity rat anti-hemagglutinin (anti-HA) monoclonal antibody (Roche Applied Science; 20 ng/ml in blocking buffer) together with a mouse anti-FLAG monoclonal antibody (Sigma; 80 ng/ml in blocking buffer) or blocking buffer alone. Secondary antibody treatment was with Alexa Fluor 594-tagged goat anti-rat IgG and Alexa Fluor 488-tagged goat anti-mouse IgG (Invitrogen; 1 μg/ml in blocking buffer) as appropriate.

RESULTS

In our earlier studies of GDP-mannose transport in *C. neoformans*, we deleted the genes encoding Gmt1 and Gmt2 in a serotype D strain background (39). The resulting *gmt1* and *gmt2* single mutants grew like the wild type in rich medium at both 30°C and 37°C (reference 39 and data not shown), although *gmt1* cells showed a modest growth defect at 37°C in the presence of the cell wall stressor calcofluor white (Fig. 1). To further define the roles of the two cryptococcal transporters in the biology of this fungal pathogen, we generated a double mutant strain in the same background. The double mutant showed only mildly reduced viability at 30°C (Fig. 1). This was surprising, given the essentiality of *VRG4*, the gene encoding the single GDP-mannose transporter in *S. cerevisiae* (12) (see Discussion). The double mutant was not viable at 37°C, however, either in the presence of 80 μg/ml calcofluor white (Fig. 1) or its absence (not shown).

GDP-mannose transport is important in fungi for the synthesis of cell wall polysaccharides (22) and mannoproteins (24), so defects in this process generally correlate with defects in cell wall integrity (12). To test this property in our strains, we examined the growth of *gmt* mutants at 30°C in the presence of SDS concentrations ranging from 0.0001% to 0.1% (Fig. 2). The single mutants responded like wild-type cells to this stressor. In contrast, the *gmt1 gmt2* double mutant was significantly more sensitive, showing only half as much growth as the other strains at 0.0025% SDS, a concentration at which the wild type and single mutants grew normally. The double mutant was also more sensitive to caffeine, sorbitol, ruthenium red, and hygromycin B (data not shown). (Addition of sorbitol to provide osmotic support did not reduce sensitivity to the other stressors [data not shown].) In all of these conditions, each single mutant behaved like the wild type.

Based on the growth defects of the double mutant, we suspected that it might have reduced virulence in a mouse model of cryptococcal infection. To test this, we generated *gmt1* and *gmt2* single and double mutants in the more virulent serotype A background (see Materials and Methods). As suspected, the double mutant was completely avirulent, although single mutants had normal virulence (Fig. 3 and data not shown).

Our results to this point suggested that Gmt1 and Gmt2 are redundant proteins involved in a key cellular process. Each protein can presumably compensate for loss of the other, but in the

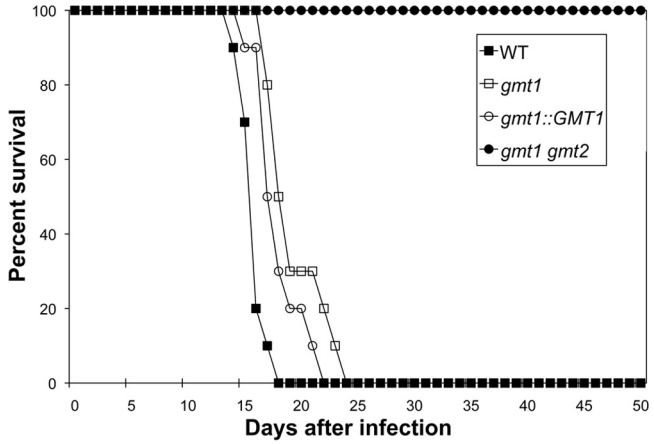

FIG 3 The *gmt1 gmt2* double mutant is severely attenuated for virulence. Mice were monitored for 50 days after inhalational inoculation with 2×10^5 cells of the indicated serotype A strains. Animals exhibiting loss of greater than or equal to 20% of body weight were humanely sacrificed.

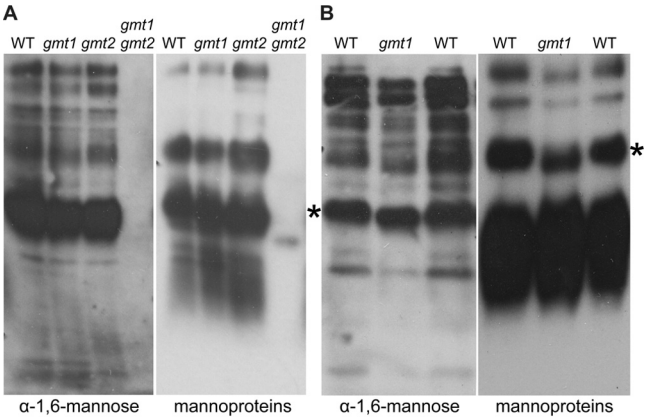

FIG 4 Single *gmt* mutations have modest effects on protein glycosylation. Total protein fractions of the strains indicated were resolved by SDS-PAGE and immmunoblotted with antibody specific for terminal α-1,6-mannose residues or mannoproteins, as indicated below. Panel A, 10% gel; panel B, 12% gel. *, examples of bands that migrate faster in *gmt1* cells; the wild type was loaded twice to facilitate comparison. For each panel, the same amount of protein was loaded in all lanes.

double mutant function is so compromised that it alters critical phenotypes. This model is consistent with our *in vitro* studies that showed similar activities of the two proteins when each was expressed individually in *S. cerevisiae* (39) and suggests that they have the same cellular function. One observation, however, led us to question this model: we had noted a growth defect in *gmt1* cells at 37°C in the presence of 80 μg/ml calcofluor white (Fig. 1) that was not evident in *gmt2*. To probe potential specific functions of the two transporters, we therefore explored additional phenotypes.

Beyond its occurrence in capsule and cell wall, mannose is a major component of both N- and O-linked glycans in yeast (2–4). We broadly surveyed protein N-glycosylation in *gmt* mutants by performing immunoblotting experiments with an antibody specific for terminal α1,6-mannose, which is added to N-glycans in the Golgi complex (2). The *gmt1 gmt2* double mutant showed a striking defect in this modification; similar results were observed when we used antiserum made against beta-eliminated cryptococcal mannoproteins (lacking O-glycans) (Fig. 4A). We also noted a modest but consistent effect on protein glycosylation in the absence of *GMT1*; several polypeptides demonstrated increased gel migration, consistent with reduced glycosylation, and the overall signal was slightly reduced compared to that of the wild type (Fig. 4B). We obtained qualitatively similar results when we probed blots with antiserum made against an *S. cerevisiae* cell wall protein (46) that cross-reacts with several cryptococcal polypeptides (data not shown). Notably, the absence of *GMT2* did not significantly change the glycosylation profile from that of the wild type in parallel studies with each antibody (data not shown). These results suggested that while both Gmt proteins act in protein glycosylation, Gmt1 plays a more important role.

We found evidence for a dominant role for Gmt1 in several contexts beyond protein glycosylation. In the course of our growth studies, we had noticed that *gmt1 gmt2* double mutant cells tended to form clumps in liquid medium. We observed a mild version of this phenotype in cultures of *gmt1*, although not in cultures of *gmt2* (Fig. 5, top panel). We also noticed a difference in colony morphology (Fig. 5, bottom panel); the *gmt1* mutant colony surface was duller than that of the wild type, while the *gmt2* mutant showed no obvious defect. Both cell clumpiness and dull colony morphology are suggestive of a defect in capsule production, as in the acapsular *cap67* mutant shown for comparison (Fig. 5). The colonies of the double mutant not only were dull but also showed a distinctly altered morphology (Fig. 5, bottom panel). The cell wall defects of this strain that are suggested by its SDS sensitivity (Fig. 2) may contribute to this phenotype.

Mannose is a major component of both of the cryptococcal capsule polysaccharides (GXM and GXMGal [32, 36, 37]), and

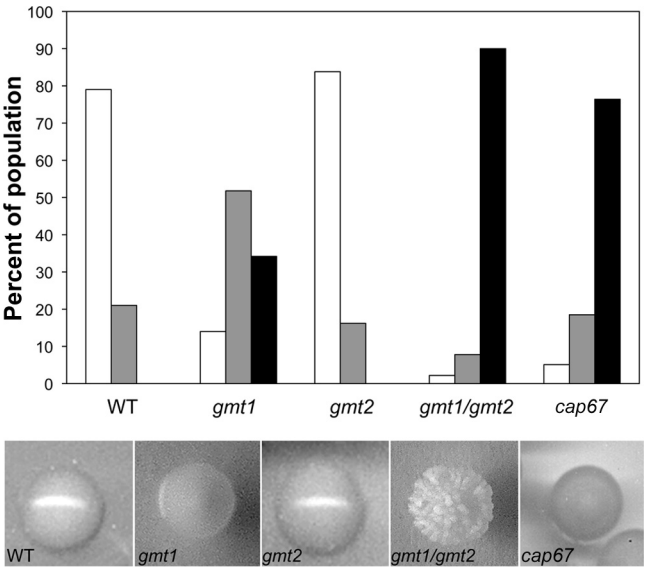

FIG 5 Cells lacking Gmt proteins have altered morphology. (Top) The indicated strains were grown in YPD, and the fraction of cells occurring as single cells (open bars), in small aggregates (2 or 3 cells, gray bars), and clumps (>3 cells, black bars) was determined. A representative experiment is shown, where at least 200 cells of each strain were categorized. (Bottom) Photographs of representative colonies of the indicated strains, grown on YPD. The light reflection seen on wild-type and *gmt2* cells indicates normal encapsulation, manifested as shiny colony morphology.

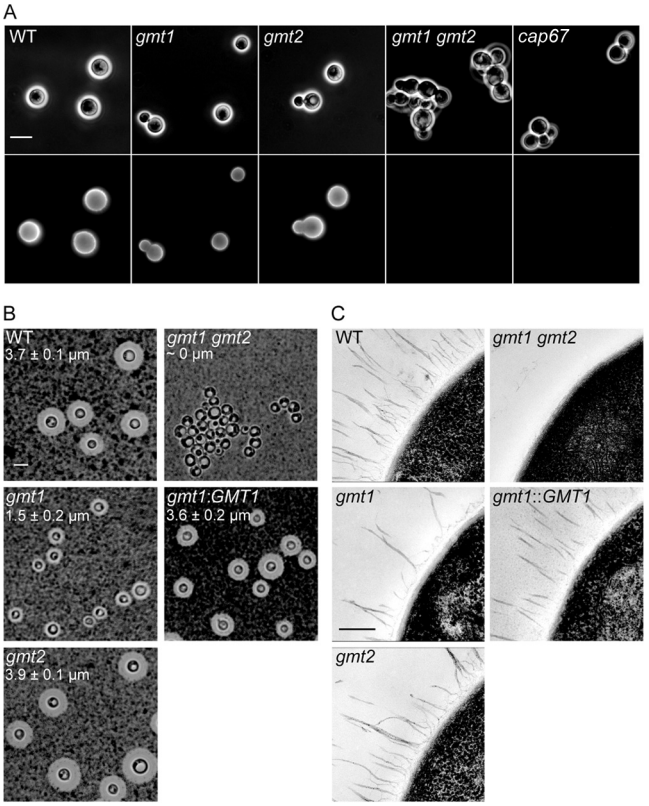

FIG 6 Capsule alteration in *gmt* mutants. (A) Antibody staining. Bright-field images of the indicated strains grown under capsule-inducing conditions and labeled with anticapsule antibody 3C2 (see Materials and Methods) (top); immunofluorescence micrographs of the same fields (bottom). Scale bar, 5 μm. (B) Negative staining. The indicated strains were grown as indicated for panel A, mixed with India ink as described in Materials and Methods, and examined by light microscopy. The average and standard deviation of the mean capsule thickness for 25 cells is indicated on each panel; this could not be assessed for the apparently acapsular and highly clumpy double mutant. Scale bar, 5 μm. (C) Electron microscopy. Each image shows part of the edge of one representative cell for the strain indicated. *gmt1*::*GMT1* denotes the *gmt1* mutant chromosomally complemented with the wild-type gene. Scale bar, 250 nm.

earlier studies have shown that the absence of GDP-mannose synthesis severely curtails capsule production (49). We previously demonstrated that GXM is synthesized in the secretory pathway (34), likely in the Golgi complex. Together, these findings imply that capsule synthesis requires the transport of GDP-mannose into the Golgi complex and therefore would need an appropriate transporter. To probe the capsule defect suggested by the dull colony and clumpy growth morphologies that we had observed, we stained our panel of mutants with a monoclonal anticapsule antibody. We noted that the *gmt1* cells stained less intensely than the wild-type and *gmt2* strains, consistent with a partial capsule defect (Fig. 6A and data not shown). Strikingly, the *gmt1 gmt2* double mutant showed no detectable fluorescent signal, suggesting a complete lack of GXM that is comparable to what is seen in an acapsular mutant (Fig. 6A).

Under certain growth conditions, including those mimicking aspects of the mammalian host environment, cryptococci generate significantly enlarged capsules (28). To assess the ability of the *gmt* mutants to upregulate capsule production, we grew the cells under capsule-inducing conditions. We then used negative staining with India ink to visualize the capsules and measured them to quantitate induction (Fig. 6B). Consistent with the experiments presented above, *gmt1* mutant cells displayed significantly reduced capsule thickness compared to that of the wild type (1.5 ± 0.2 μm versus 3.7 ± 0.1 μm; $P < 0.05$); complementation of this mutant with the wild-type *GMT1* gene restored it to wild-type thickness (3.6 ± 0.2 μm; $P = 0.4$). Capsules of *gmt2* cells were also similar to those of wild-type cells (3.9 ± 0.1 μm; $P = 0.2$), while the capsules of *gmt1 gmt2* double mutant cells were undetectable, even under these inducing conditions.

The thickness of the capsule, which reflects fiber length (50, 51), was clearly reduced in *gmt1* mutants, but these studies did not address fiber density. To investigate this, we performed electron microscopy (Fig. 6C). We noted that *gmt1* fibers were markedly more sparse than those of the wild type, although the complemented *gmt1* mutant and *gmt2* cells looked normal in this respect. Consistent with our observations by light microscopy, we detected no capsule fibers on the surfaces of *gmt1 gmt2* double mutant cells.

Our results suggested that in contrast to cell wall integrity phenotypes, where the two transporters seem to effectively compensate for one another, normal growth at 37°C, protein N-glycosylation, and capsule synthesis all rely more heavily on the activity of Gmt1 and are dramatically impaired in the absence of both proteins (see Discussion). Because of the similar *in vitro* activities of these proteins (39), we suspected that the apparent difference in protein function was due to levels of expression. We therefore evaluated gene expression by RNA-Seq at various time points of capsule induction. This study showed significantly higher expression of *GMT1*, which ranged from roughly 3-fold that of *GMT2* in rich medium (YPD, zero time in Fig. 7) to over 25-fold after 1 day under capsule-inducing conditions (24 h in Fig. 7).

To confirm our hypothesis that the phenotypic differences between *gmt1* and *gmt2* reflected the distinct expression levels of their remaining *GMT* genes, we performed a gene swap experiment, diagrammed in Fig. 8 (panel A). To do this, we replaced the wild-type *GMT* gene that remained in each single mutant with the absent coding sequence. This generated pairs of strains expressing the same gene from different genomic contexts (*GMT2* in strains 2 and 5; *GMT1* in strains 3 and 4). When we measured *GMT* gene expression in these strains by qRT-PCR, we noticed that absence of either *GMT* did not significantly alter expression of the other (Fig. 8C; compare strains 2 and 3 to strain 1). This suggests that there is no mechanism for compensatory upregulation of either *GMT* upon loss of the other. We also noted that movement of *GMT1* from its native locus (strain 3) to the *GMT2* locus (strain 4) reduced its expression roughly 25-fold, consistent with the RNA-Seq expression differences between these loci that we observed in wild-type cells under the same inducing conditions (Fig. 7). The change in *GMT2* expression between the two sites, however, was significantly less (roughly 3-fold; compare strains 2 and 5), although in the expected direction.

We next assessed capsule induction by negative staining after growth under inducing conditions. We found that moving *GMT1* to the usual site of *GMT2* caused reduced *GMT1* expression and dramatic reduction in capsule thickness (Fig. 8B and C; compare strains 3 and 4). Furthermore, moving *GMT2* to the usual site of *GMT1* caused an increase in gene expression and capsule size (compare strains 2 and 5). These data are consistent with a model of interchangeable transporters, which differ only in expression

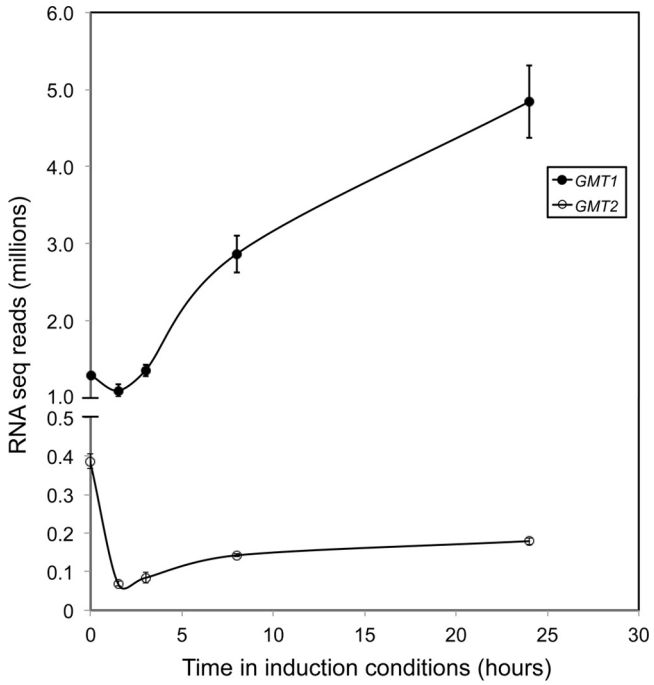

FIG 7 *GMT* gene expression in wild-type cells under capsule induction conditions. Wild-type KN99α cells were grown under capsule-inducing conditions, and RNA-Seq analysis was performed at 0, 1.5, 3, 8, and 24 h. The expression values plotted (median ± standard deviation) were calculated from three separate experiments, each including RNA prepared from three biological replicate cultures.

level. However, comparison of strains with different genes in the same site as their sole *GMT* sequences suggests otherwise. For example, expressing *GMT2* from the *GMT1* locus (strain 5) yielded consistently smaller capsules than when the endogenous gene was at that site (strain 3): even expressed at levels similar to those expected for *GMT1*, *GMT2* did not functionally replace it.

The capsule thickness of each strain (Fig. 8B) generally correlated with total expression of *GMT* sequences (Fig. 8C), and the two strains with the lowest *GMT* expression (and least capsule) showed cell and colony morphology consistent with clumpy acapsular cells (Fig. 8B and D, strains 4 and 6). To our surprise, however, the growth of the various strains on rich medium (Fig. 8D) did not similarly correlate with *GMT* expression under those growth conditions (see Fig. S1 in the supplemental material, top panel). In particular, colonies of strain 5, where *GMT2* was expressed from a nonnative locus, grew slowly (note the small colony size in Fig. 8D) despite robust *GMT2* expression in this medium (see Fig. S1 in the supplemental material, top panel); it may be that this level of *GMT2* expression is toxic to the cells (see Discussion). Furthermore, both of the swapped strains (4 and 5) were highly sensitive to SDS stress, resembling the double mutant in rich medium (see Fig. S1 in the supplemental material, bottom panel). This was the case even though *GMT1* expression from strain 4 was close to *GMT2* expression in strain 2 and *GMT2* expression in strain 5 exceeded *GMT1* expression in strain 3 (see Fig. S1 in the supplemental material, top panel). These observations held in multiple independent transformants.

The results of our gene swapping study suggested that factors beyond gene expression influence Gmt function: despite similar activity *in vitro* in an exogenous system, these proteins do not appear to function identically *in vivo* even when expressed from

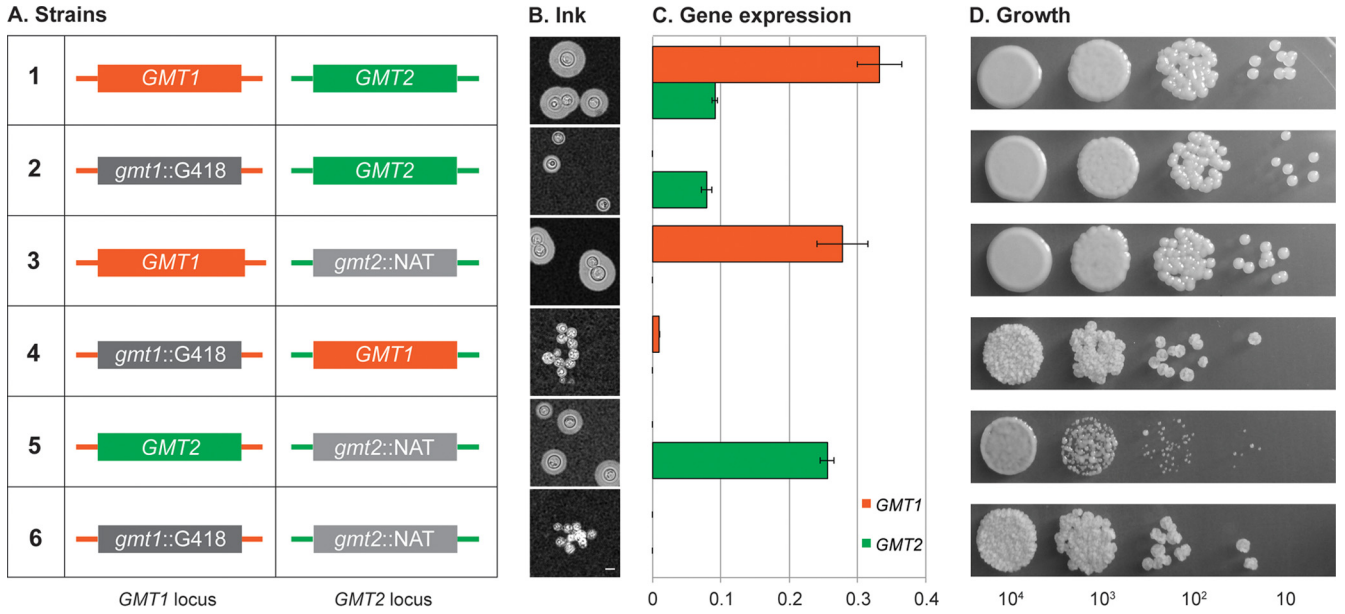

FIG 8 Genomic location does not explain the functional differences between *GMT1* and *GMT2*. (A) Schematic representation of the *GMT* strain variants listed at left, indicating the coding sequence present at each locus (colored boxes): orange, *GMT1*; green, *GMT2*; dark gray, Geneticin resistance marker (G418) replacing *GMT1* (*gmt1*::G418); light gray, nourseothricin resistance marker (NAT) replacing *GMT2* (*gmt2*::NAT). Promoter and terminator sequences of each locus (colored lines) were not altered. Strains: 1, wild type; 2, *gmt1* mutant; 3, *gmt2* mutant; 4 and 5, new "swapped" strains; 6, *gmt1 gmt2* double mutant. (B) The capsule thickness of each strain under capsule-inducing conditions was examined with India ink as described in Materials and Methods. Scale bar, 5 μm. (C) *GMT* expression levels under capsule-inducing conditions determined by RT-PCR, plotted relative to *ACT1*. (D) Growth on rich medium. Aliquots (5 μl) of a stock cell suspension (2×10^6 cells/ml) and three 10-fold serial dilutions were spotted on YPD plates and grown for 1 day at 30°C.

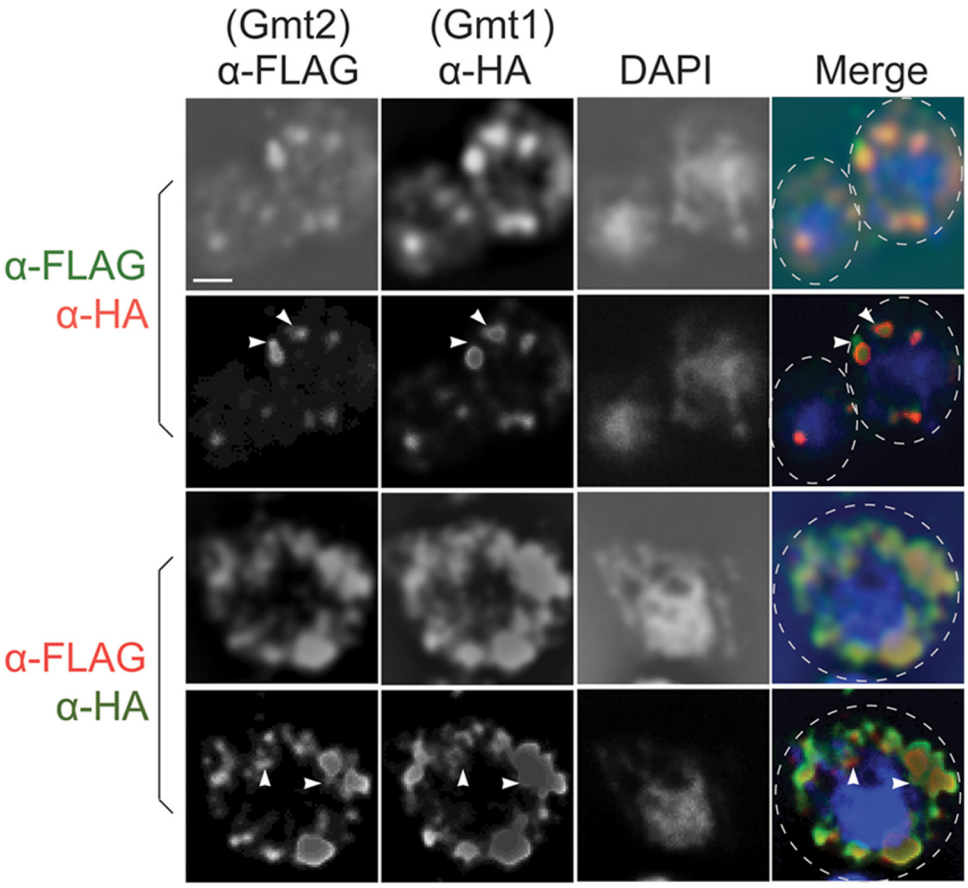

FIG 9 Gmt proteins are located in the Golgi complex. Chromosomally expressed Gmt1-HA and Gmt2-Flag were immunolocalized and imaged as detailed in the text. Shown are single-channel and merged images of signal derived from staining with DAPI (4′,6-diamidino-2-phenylindole) (nucleus) and with antibodies to the two tags as indicated. Arrowheads indicate examples of regions where Gmt1 and Gmt2 do not colocalize; broken white lines indicate the cell edge as observed under bright-field microscopy. Scale bar, 5 μm.

the same locus at similar levels. One possible explanation is that the proteins are differentially localized. Because both Gmt1 and Gmt2 complement the loss of *S. cerevisiae* Vrg4p (39), which is known to be a Golgi protein (13), we had assumed them to be similarly localized. However, there is precedent for subcompartmentalization of Golgi functions (52) and for association of nucleotide sugar transporters with specific glycosyltransferases (53).

To examine the localization of the Gmt1 and Gmt2 proteins by immunofluorescence microscopy, we modified the chromosomal copies of *GMT1* and *GMT2* to encode C-terminally epitope-tagged proteins (Gmt1-HA and Gmt2-FLAG); we know from our previous studies that C-terminally modified GMTs are still functional (39). When we probed the resulting doubly tagged strain with both anti-HA and anti-FLAG antibodies, we observed staining of large puncta in a perinuclear distribution, consistent with Golgi localization (4, 13). Neither protein colocalized with BiP, a marker of the endoplasmic reticulum (not shown). To improve resolution, we used AxioVision 4.8 software (Carl Zeiss) for image deconvolution. Images processed by an inverse filter algorithm (Fig. 9, first row) showed that the two Gmt proteins generally colocalized, although occasional areas where only one was stained were also detectable (Fig. 9 and data not shown). Application of a fast iterative algorithm resulted in sharper images but with lower total signal intensity (Fig. 9, second row, and data not shown). In such images, we could clearly appreciate the membrane localization of the two Gmt proteins, as well as regions where they did not completely colocalize (examples indicated by arrowheads); interestingly, the latter consistently gave the impression that regions of Gmt1 staining surrounded those of Gmt2 localization (Fig. 9 and data not shown). This result held even when the secondary antibody fluorophores were swapped to rule out potential artifacts due to staining or fluorophore properties (Fig. 9, third and fourth rows).

DISCUSSION

C. neoformans has two functional GDP-mannose transporters, which show the same biochemical activity *in vitro* (39). Surprisingly, cells lacking both of these proteins grow well, although they are somewhat compromised in growth under stress (Fig. 1 and 2). This contrasts with findings in *S. cerevisiae* and most other fungi that have been tested, where GDP-mannose transport is essential (12, 21, 23, 24). *A. fumigatus* is notably also viable without its single GDP-mannose transporter, but the mutant is severely defective in growth and cannot spread or sporulate (22). There are several possible explanations for the robustness of *C. neoformans gmt1 gmt2* cells. One is that Golgi glycan synthetic reactions involving mannose, such as the extension of protein-linked glycans, are not needed for cryptococcal viability or virulence. This is con-

sistent with the findings of Park et al. in studies of *C. neoformans* mutants unable to initiate Golgi α-1,6-mannose branching (3). In this regard, it is also notable that cryptococcal N-glycan extension is more limited than that of *S. cerevisiae* or *C. albicans* (2); this is also the case for *A. fumigatus* (54). Another possibility is that other *C. neoformans* nucleotide sugar transporters that are localized to the Golgi complex have sufficiently relaxed specificity to transport some amount of GDP-mannose. Our finding that protein N-glycans in *gmt1 gmt2* cells are apparently devoid of the terminal α-1,6-mannose modification that is normally acquired in the Golgi complex (Fig. 4A) argues against this, but additional glycan analysis will be required to resolve this question.

Gmt1 and Gmt2 behave similarly in terms of *in vitro* assays and complementation of an *S. cerevisiae* mutant defective in GDP-mannose transport (39). However, the *gmt1* and *gmt2* single mutants have distinct phenotypes, with greater or lesser differences from the wild type depending on the biological process queried. In some cases, both single mutants resemble the wild type, as with cell wall integrity (Fig. 2) or virulence (Fig. 3 and data not shown). In others, the two single mutants exhibit modest differences; an example of this is protein glycosylation, where a size shift suggesting reduced terminal glycan modification is seen in a subset of *gmt1* polypeptides but not seen in *gmt2* polypeptides (Fig. 4B and data not shown). There are also striking differences between the two mutants. For example, *gmt1* cells show significant reduction in capsule thickness and fiber density compared to the wild type. These capsule defects are reflected in colony appearance and cell clumping in culture and cannot be overcome by capsule-inducing conditions. In contrast, capsule is normal in *gmt2* cells by all of these tests. Distinct phenotypes have also been observed in *A. nidulans* mutants lacking one of a pair of GDP-mannose transporter genes (25, 26), although a double mutant in that system has not been reported.

We initially postulated that the activities of Gmt1 and Gmt2 are simply redundant, which would be consistent with the more extreme defects of cells lacking both transporters. In this case, the different single mutant phenotypes could reflect differential expression of the two proteins, as has been suggested for *A. nidulans* (25, 26). In line with this idea, our RNA-Seq results indicate that *GMT1* mRNA expression is severalfold higher than that of *GMT2* in rich medium and rises to 1 order of magnitude higher under capsule-inducing conditions. Immunostaining and immunoblotting studies (not shown) also suggested that Gmt1 is also more abundant at the protein level, although in those experiments the two proteins bore different epitope tags, so the comparison is not definitive. In this model, the lack of the more abundant protein, Gmt1, would be expected to have more dramatic consequences, as we do observe for several phenotypes that we tested. The differing effects on various biosynthetic processes seen in each mutant might then reflect cellular prioritization of glycan synthetic pathways in the context of enzymatic competition for use of a limited resource (Golgi complex-localized GDP-mannose). Alternatively, the differing extents of perturbation of various cellular processes could parallel the overall demand for GDP-mannose: capsule production under inducing conditions, for example, likely requires more mannose than does N-glycan outer chain modification.

Although a model of completely redundant activities is consistent with many of our results, it raises the question of why *C. neoformans* and its sister species *Cryptococcus gattii*, which diverged over 45 million years ago, have each maintained two copies of this transporter. Furthermore, simple movement of each gene to the genomic location of the other did not yield the phenotypes that would be expected from the resulting modulation of RNA expression levels if the gene products behaved identically (Fig. 8); overexpression of *GMT2* also did not complement the defects in *gmt1* mutant cells (data not shown). These studies suggest an alternative model, whereby the two transporters in fact play different roles, although they can compensate for each other to a certain extent in the setting of single mutants. This hypothesis is supported by the distinct expression patterns of the two genes across multiple growth conditions (39), including opposite responses to capsule-inducing conditions (Fig. 7). The higher substrate affinity of Gmt2, which has a K_m for GDP-mannose that is twice that of Gmt1 (39), also suggests distinct functions of the two proteins, as does our observation that when *GMT2* is expressed at *GMT1* levels (Fig. 8, strain 5), it has adverse effects on cell growth (Fig. 8D and Fig. S1 in the supplemental material); potentially Gmt2 directs substrate to less productive biosynthetic pathways. Interestingly, the two Gmt proteins in *A. nidulans* also demonstrate different expression patterns that suggest distinct roles in development (26).

Our imaging studies (Fig. 9) hint that although the two transporters largely colocalize, they may also occur in distinct locations within the secretory pathway. This could in turn enable association with distinct glycosyltransferases or synthetic complexes that mediate specific cellular functions and may also influence protein stability. Reports from studies of mammals, yeasts, insects, and plants suggest that subcompartmentalization contributes to efficient organization of glycan synthesis in eukaryotes (52, 55, 56). Defining such compartments in *C. neoformans*, however, will require resolution beyond those of the methods that we have employed (standard immunofluorescence with deconvolution software) because of the limits imposed by the size of this yeast and its organelle structure; newer microscopy approaches, such as stochastic optical reconstruction microscopy (STORM) (57), may be required for these studies.

We did consider the possibility that Gmt1 and Gmt2 interact with each other. The Vrg4 protein in *S. cerevisiae* dimerizes, which is important for its GDP-Man transport activity (58, 59), and the LPG2 GDP-mannose transporter of *Leishmania* functions as a homohexamer (60). Preliminary studies (not shown) did not reveal such interactions. Furthermore, the differing regulation and relative abundance of the two transcripts and the similar phenotypes of wild type and *gmt2* cells argue against this model. Nonetheless, we cannot strictly rule out this possibility.

It is notable that *gmt1* cells do not show a significant defect in virulence, despite reduced capsule and several underglycosylated proteins. It appears that the mutant yeast cells, which do maintain some capsule, are able to sufficiently balance glycan synthetic processes *in vivo* to compensate for reduced mannose utilization. The double mutant strain, in contrast, clearly demonstrates the critical role of mannose glycosylation in *C. neoformans*. This strain is sensitive to stress and temperature, has incomplete N-glycans, is essentially acapsular, and is avirulent in a mouse model of infection. The lack of virulence of the double mutant, coupled with the fact that humans and other mammalian hosts of *C. neoformans* do not express GDP-mannose transporters, suggests these proteins as potential targets for antifungal chemotherapy.

ACKNOWLEDGMENTS

We are grateful to Tom Kozel, Stuart Levitz, and Randy Schekman for antibodies used in these studies and to Jeffrey Brodsky for anti-BiP antibody used in experiments cited but not shown. We thank Wandy Beatty for advice on microscopy methods and interpretation and Brian Haynes for discussion of RNA-Seq data. We also appreciate helpful discussions with members of the Doering lab and thank Felipe Santiago and Lucy Li for comments on the manuscript.

These studies were supported by NIH grants GM071007, GM066303, and AI087794.

REFERENCES

1. **Lowe JB, Marth JD.** 2003. A genetic approach to mammalian glycan function. Annu. Rev. Biochem. **72:**643–691. http://dx.doi.org/10.1146/annurev.biochem.72.121801.161809.
2. **Gemmill TR, Trimble RB.** 1999. Overview of N- and O-linked oligosaccharide structures found in various yeast species. Biochim. Biophys. Acta **1426:**227–237. http://dx.doi.org/10.1016/S0304-4165(98)00126-3.
3. **Park JN, Lee DJ, Kwon O, Oh DB, Bahn YS, Kang HA.** 2012. Unraveling unique structure and biosynthesis pathway of N-linked glycans in human fungal pathogen *Cryptococcus neoformans* by glycomics analysis. J. Biol. Chem. **287:**19501–19515. http://dx.doi.org/10.1074/jbc.M112.354209.
4. **Reilly MC, Aoki K, Wang ZA, Skowyra ML, Williams M, Tiemeyer M, Doering TL.** 2011. A xylosylphosphotransferase of *Cryptococcus neoformans* acts in protein O-glycan synthesis. J. Biol. Chem. **286:**26888–26899. http://dx.doi.org/10.1074/jbc.M111.262162.
5. **Klis FM, Boorsma A, De Groot PW.** 2006. Cell wall construction in *Saccharomyces cerevisiae*. Yeast **23:**185–202. http://dx.doi.org/10.1002/yea.1349.
6. **Orlean P, Menon AK.** 2007. Thematic review series: lipid posttranslational modifications. GPI anchoring of protein in yeast and mammalian cells, or: how we learned to stop worrying and love glycophospholipids. J. Lipid Res. **48:**993–1011. http://dx.doi.org/10.1194/jlr.R700002-JLR200.
7. **Freeze HH, Elbein AD.** 2009. Glycosylation precursors, chapter 4, p 47–61. *In* Varki A, Cummings RD, Esko JD, Freeze H, Stanley P, Bertozzi CR, Hart GW, Etzler ME (ed), Essentials of glycobiology, 2nd ed. Cold Spring Harbor Press, Cold Spring Harbor, NY.
8. **Helenius J, Aebi M.** 2002. Transmembrane movement of dolichol linked carbohydrates during N-glycoprotein biosynthesis in the endoplasmic reticulum. Semin. Cell Dev. Biol. **13:**171–178. http://dx.doi.org/10.1016/S1084-9521(02)00045-9.
9. **Liu L, Xu YX, Hirschberg CB.** 2010. The role of nucleotide sugar transporters in development of eukaryotes. Semin. Cell Dev. Biol. **21:**600–608. http://dx.doi.org/10.1016/j.semcdb.2010.02.002.
10. **Gerardy-Schahn R, Oelmann S, Bakker H.** 2001. Nucleotide sugar transporters: biological and functional aspects. Biochimie **83:**775–782. http://dx.doi.org/10.1016/S0300-9084(01)01322-0.
11. **Abeijon C, Orlean P, Robbins PW, Hirschberg CB.** 1989. Topography of glycosylation in yeast: characterization of GDPmannose transport and lumenal guanosine diphosphatase activities in Golgi-like vesicles. Proc. Natl. Acad. Sci. U. S. A. **86:**6935–6939. http://dx.doi.org/10.1073/pnas.86.18.6935.
12. **Poster JB, Dean N.** 1996. The yeast *VRG4* gene is required for normal Golgi functions and defines a new family of related genes. J. Biol. Chem. **271:**3837–3845. http://dx.doi.org/10.1074/jbc.271.7.3837.
13. **Dean N, Zhang YB, Poster JB.** 1997. The *VRG4* gene is required for GDP-mannose transport into the lumen of the Golgi in the yeast, *Saccharomyces cerevisiae*. J. Biol. Chem. **272:**31908–31914. http://dx.doi.org/10.1074/jbc.272.50.31908.
14. **Baldwin TC, Handford MG, Yuseff MI, Orellana A, Dupree P.** 2001. Identification and characterization of GONST1, a Golgi-localized GDP-mannose transporter in Arabidopsis. Plant Cell **13:**2283–2295. http://dx.doi.org/10.1105/tpc.13.10.2283, http://dx.doi.org/10.2307/3871508.
15. **Ueki N, Nishii I.** 2009. Controlled enlargement of the glycoprotein vesicle surrounding a *volvox* embryo requires the InvB nucleotide-sugar transporter and is required for normal morphogenesis. Plant Cell **21:**1166–1181. http://dx.doi.org/10.1105/tpc.109.066159.
16. **Handford MG, Sicilia F, Brandizzi F, Chung JH, Dupree P.** 2004. *Arabidopsis thaliana* expresses multiple Golgi-localised nucleotide-sugar transporters related to GONST1. Mol. Genet. Genomics **272:**397–410. http://dx.doi.org/10.1007/s00438-004-1071-z.
17. **Ma D, Russell DG, Beverley SM, Turco SJ.** 1997. Golgi GDP-mannose uptake requires Leishmania LPG2. A member of a eukaryotic family of putative nucleotide-sugar transporters. J. Biol. Chem. **272:**3799–3805.
18. **Descoteaux A, Luo Y, Turco SJ, Beverley SM.** 1995. A specialized pathway affecting virulence glycoconjugates of *Leishmania*. Science **269:**1869–1872. http://dx.doi.org/10.1126/science.7569927.
19. **Ballou L, Hitzeman RA, Lewis MS, Ballou CE.** 1991. Vanadate-resistant yeast mutants are defective in protein glycosylation. Proc. Natl. Acad. Sci. U. S. A. **88:**3209–3212. http://dx.doi.org/10.1073/pnas.88.8.3209.
20. **Arakawa K, Abe M, Noda Y, Adachi H, Yoda K.** 2006. Molecular cloning and characterization of a *Pichia pastoris* ortholog of the yeast Golgi GDP-mannose transporter gene. J. Gen. Appl. Microbiol. **52:**137–145. http://dx.doi.org/10.2323/jgam.52.137.
21. **Carvalho ND, Arentshorst M, Weenink XO, Punt PJ, van den Hondel CA, Ram AF.** 2011. Functional YFP-tagging of the essential GDP-mannose transporter reveals an important role for the secretion related small GTPase SrgC protein in maintenance of Golgi bodies in *Aspergillus niger*. Fungal Biol. **115:**253–264. http://dx.doi.org/10.1016/j.funbio.2010.12.010.
22. **Engel J, Schmalhorst PS, Routier FH.** 2012. Biosynthesis of the fungal cell wall polysaccharide galactomannan requires intraluminal GDP-mannose. J. Biol. Chem. **287:**44418–44424. http://dx.doi.org/10.1074/jbc.M112.398321.
23. **Nishikawa A, Mendez B, Jigami Y, Dean N.** 2002. Identification of a *Candida glabrata* homologue of the *S. cerevisiae VRG4* gene, encoding the Golgi GDP-mannose transporter. Yeast **19:**691–698. http://dx.doi.org/10.1002/yea.854.
24. **Nishikawa A, Poster JB, Jigami Y, Dean N.** 2002. Molecular and phenotypic analysis of *CaVRG4*, encoding an essential Golgi apparatus GDP-mannose transporter. J. Bacteriol. **184:**29–42. http://dx.doi.org/10.1128/JB.184.1.29-42.2002.
25. **Jackson-Hayes L, Hill TW, Loprete DM, Fay LM, Gordon BS, Nkashama SA, Patel RK, Sartain CV.** 2008. Two GDP-mannose transporters contribute to hyphal form and cell wall integrity in *Aspergillus nidulans*. Microbiology **154:**2037–2047. http://dx.doi.org/10.1099/mic.0.2008/017483-0.
26. **Jackson-Hayes L, Hill TW, Loprete DM, Gordon BS, Groover CJ, Johnson LR, Martin SA.** 2010. GDP-mannose transporter paralogues play distinct roles in polarized growth of *Aspergillus nidulans*. Mycologia **102:**305–310. http://dx.doi.org/10.3852/09-138.
27. **Park BJ, Wannemuehler KA, Marston BJ, Govender N, Pappas PG, Chiller TM.** 2009. Estimation of the current global burden of cryptococcal meningitis among persons living with HIV/AIDS. AIDS **23:**525–530. http://dx.doi.org/10.1097/QAD.0b013e328322ffac.
28. **Doering TL.** 2009. How sweet it is! Cell wall biogenesis and polysaccharide capsule formation in *Cryptococcus neoformans*. Annu. Rev. Microbiol. **63:**223–247. http://dx.doi.org/10.1146/annurev.micro.62.081307.162753.
29. **Heise N, Gutierrez AL, Mattos KA, Jones C, Wait R, Previato JO, Mendonca-Previato L.** 2002. Molecular analysis of a novel family of complex glycoinositolphosphoryl ceramides from *Cryptococcus neoformans*: structural differences between encapsulated and acapsular yeast forms. Glycobiology **12:**409–420. http://dx.doi.org/10.1093/glycob/cwf053.
30. **Olson GM, Fox DS, Wang P, Alspaugh JA, Buchanan KL.** 2007. Role of protein O-mannosyltransferase Pmt4 in the morphogenesis and virulence of *Cryptococcus neoformans*. Eukaryot. Cell **6:**222–234. http://dx.doi.org/10.1128/EC.00182-06.
31. **Kumar P, Yang M, Haynes BC, Skowyra ML, Doering TL.** 2011. Emerging themes in cryptococcal capsule synthesis. Curr. Opin. Struct. Biol. **21:**597–602. http://dx.doi.org/10.1016/j.sbi.2011.08.006.
32. **Cherniak R, Valafar H, Morris LC, Valafar F.** 1998. *Cryptococcus neoformans* chemotyping by quantitative analysis of ^{1}H nuclear magnetic resonance spectra of glucuronoxylomannans with a computer-simulated artificial neural network. Clin. Diagn. Lab. Immunol. **5:**146–159.
33. **Chang YC, Kwon-Chung KJ.** 1994. Complementation of a capsule-deficient mutation of *Cryptococcus neoformans* restores its virulence. Mol. Cell. Biol. **14:**4912–4919.
34. **Yoneda A, Doering TL.** 2006. A eukaryotic capsular polysaccharide is synthesized intracellularly and secreted via exocytosis. Mol. Biol. Cell **17:**5131–5140. http://dx.doi.org/10.1091/mbc.E06-08-0701.
35. **Zaragoza O, Rodrigues ML, De Jesus M, Frases S, Dadachova E, Casadevall A.** 2009. The capsule of the fungal pathogen *Cryptococcus neoformans*. Adv. Appl. Microbiol. **68:**133–216. http://dx.doi.org/10.1016/S0065-2164(09)01204-0.

36. **Vaishnav VV, Bacon BE, O'Neill M, Cherniak R.** 1998. Structural characterization of the galactoxylomannan of *Cryptococcus neoformans* Cap67. Carbohydr. Res. **306:**315–330.
37. **Heiss C, Klutts JS, Wang Z, Doering TL, Azadi P.** 2009. The structure of *Cryptococcus neoformans* galactoxylomannan contains beta-D-glucuronic acid. Carbohydr. Res. **344:**915–920.
38. **Heiss C, Skowyra ML, Liu H, Klutts JS, Wang Z, Williams M, Srikanta D, Beverley SM, Azadi P, Doering TL.** 2013. Unusual galactofuranose modification of a capsule polysaccharide in the pathogenic yeast *Cryptococcus neoformans*. J. Biol. Chem. **288:**10994–1003. http://dx.doi.org/10.1074/jbc.M112.441998.
39. **Cottrell TR, Griffith CL, Liu H, Nenninger AA, Doering TL.** 2007. The pathogenic fungus *Cryptococcus neoformans* expresses two functional GDP-mannose transporters with distinct expression patterns and roles in capsule synthesis. Eukaryot. Cell **6:**776–785. http://dx.doi.org/10.1128/EC.00015-07.
40. **Hua J, Meyer JD, Lodge JK.** 2000. Development of positive selectable markers for the fungal pathogen *Cryptococcus neoformans*. Clin. Diagn. Lab. Immunol. **7:**125–128.
41. **Reilly MC, Levery SB, Castle SA, Klutts JS, Doering TL.** 2009. A novel xylosylphosphotransferase activity discovered in *Cryptococcus neoformans*. J. Biol. Chem. **284:**36118–36127. http://dx.doi.org/10.1074/jbc.M109.056226.
42. **Fu J, Hettler E, Wickes BL.** 2006. Split marker transformation increases homologous integration frequency in *Cryptococcus neoformans*. Fungal Genet. Biol. **43:**200–212. http://dx.doi.org/10.1016/j.fgb.2005.09.007.
43. **McDade HC, Cox GM.** 2001. A new dominant selectable marker for use in Cryptococcus neoformans. Med. Mycol. **39:**151–154. http://dx.doi.org/10.1080/mmy.39.1.151.154.
44. **Bose I, Doering TL.** 2011. Efficient implementation of RNA interference in the pathogenic yeast Cryptococcus neoformans. J. Microbiol. Methods **86:**156–159. http://dx.doi.org/10.1016/j.mimet.2011.04.014.
45. **Franzusoff A, Schekman R.** 1989. Functional compartments of the yeast Golgi apparatus are defined by the *sec7* mutation. EMBO J. **8:**2695–2702.
46. **Kuehn MJ, Schekman R, Ljungdahl PO.** 1996. Amino acid permeases require COPII components and the ER resident membrane protein Shr3p for packaging into transport vesicles in vitro. J. Cell Biol. **135:**585–595.
47. **Haynes BC, Skowyra ML, Spencer SJ, Gish SR, Williams M, Held EP, Brent MR, Doering TL.** 2011. Toward an integrated model of capsule regulation in *Cryptococcus neoformans*. PLoS Pathog. **7:**e1002411. http://dx.doi.org/10.1371/journal.ppat.1002411.
48. **Griffith CL, Klutts JS, Zhang L, Levery SB, Doering TL.** 2004. UDP-glucose dehydrogenase plays multiple roles in the biology of the pathogenic fungus *Cryptococcus neoformans*. J. Biol. Chem. **279:**51669–51676. http://dx.doi.org/10.1074/jbc.M408889200.
49. **Wills EA, Roberts IS, Del Poeta M, Rivera J, Casadevall A, Cox GM, Perfect JR.** 2001. Identification and characterization of the *Cryptococcus neoformans* phosphomannose isomerase-encoding gene, *MAN1*, and its impact on pathogenicity. Mol. Microbiol. **40:**610–620. http://dx.doi.org/10.1046/j.1365-2958.2001.02401.x.
50. **Yoneda A, Doering TL.** 2008. Regulation of *Cryptococcus neoformans* capsule size is mediated at the polymer level. Eukaryot. Cell **7:**546–549. http://dx.doi.org/10.1128/EC.00437-07.
51. **Frases S, Pontes B, Nimrichter L, Viana NB, Rodrigues ML, Casadevall A.** 2009. Capsule of *Cryptococcus neoformans* grows by enlargement of polysaccharide molecules. Proc. Natl. Acad. Sci. U. S. A. **106:**1228–1233. http://dx.doi.org/10.1073/pnas.0808995106.
52. **Puthenveedu MA, Linstedt AD.** 2005. Subcompartmentalizing the Golgi apparatus. Curr. Opin. Cell Biol. **17:**369–375. http://dx.doi.org/10.1016/j.ceb.2005.06.006.
53. **Sprong H, Degroote S, Nilsson T, Kawakita M, Ishida N, van der Sluijs P, van Meer G.** 2003. Association of the Golgi UDP-galactose transporter with UDP-galactose:ceramide galactosyltransferase allows UDP-galactose import in the endoplasmic reticulum. Mol. Biol. Cell **14:**3482–3493. http://dx.doi.org/10.1091/mbc.E03-03-0130.
54. **Kotz A, Wagener J, Engel J, Routier FH, Echtenacher B, Jacobsen I, Heesemann J, Ebel F.** 2010. Approaching the secrets of N-glycosylation in Aspergillus fumigatus: characterization of the AfOch1 protein. PLoS One **5:**e15729. http://dx.doi.org/10.1371/journal.pone.0015729.
55. **Yamamoto-Hino M, Abe M, Shibano T, Setoguchi Y, Awano W, Ueda R, Okano H, Goto S.** 2012. Cisterna-specific localization of glycosylation-related proteins to the Golgi apparatus. Cell Struct. Funct **37:**55–63. http://dx.doi.org/10.1247/csf.11037.
56. **Schoberer J, Strasser R.** 2011. Sub-compartmental organization of Golgi-resident N-glycan processing enzymes in plants. Mol. Plant **4:**220–228. http://dx.doi.org/10.1093/mp/ssq082.
57. **Kamiyama D, Huang B.** 2012. Development in the STORM. Dev. Cell **23:**1103–1110. http://dx.doi.org/10.1016/j.devcel.2012.10.003.
58. **Abe M, Hashimoto H, Yoda K.** 1999. Molecular characterization of Vig4/Vrg4 GDP-mannose transporter of the yeast *Saccharomyces cerevisiae*. FEBS Lett. **458:**309–312.
59. **Gao XD, Dean N.** 2000. Distinct protein domains of the yeast Golgi GDP-mannose transporter mediate oligomer assembly and export from the endoplasmic reticulum. J. Biol. Chem. **275:**17718–17727. http://dx.doi.org/10.1074/jbc.M909946199.
60. **Hong K, Ma D, Beverley SM, Turco SJ.** 2000. The Leishmania GDP-mannose transporter is an autonomous, multi-specific, hexameric complex of LPG2 subunits. Biochemistry **39:**2013–2022. http://dx.doi.org/10.1021/bi992363l.
61. **Nielsen K, Cox GM, Wang P, Toffaletti DL, Perfect JR, Heitman J.** 2003. Sexual cycle of *Cryptococcus neoformans var. grubii* and virulence of congenic a and alpha isolates. Infect. Immun. **71:**4831–4841. http://dx.doi.org/10.1128/IAI.71.9.4831-4841.2003.
62. **Kwon-Chung KJ, Wickes BL, Stockman L, Roberts GD, Ellis D, Howard DH.** 1992. Virulence, serotype, and molecular characteristics of environmental strains of *Cryptococcus neoformans* var. *gattii*. Infect. Immun. **60:**1869–1874.